

Thermodynamic and electrostatic analysis of threading dislocations in epitaxial ferroelectric films

I. B. Misirlioglu, S. P. Alpay,^{a)} and M. Aindow

Department of Materials Science & Engineering and Institute of Materials Science, University of Connecticut, Storrs, Connecticut 06269

V. Nagarajan

School of Materials Science and Engineering, University of New South Wales, Sydney NSW 2052, Australia

(Received 23 September 2005; accepted 11 January 2006; published online 10 March 2006)

The role of threading dislocations on the electrical properties of epitaxial ferroelectric films is analyzed using a thermodynamic formalism and basic electrostatics. The modeling is carried out for a 300 nm thick (001) $\text{PbZr}_{0.2}\text{Ti}_{0.8}\text{O}_3$ on (001) SrTiO_3 which displays a large population of threading dislocations as determined by transmission electron microscopy. Results show that although the phase transformation characteristics of ferroelectric films containing threading dislocations are altered such that the transformation is “smeared” over a temperature interval due to local strain variations, these defects do not have as profound an effect on the electrical properties as the misfit dislocations. © 2006 American Institute of Physics. [DOI: 10.1063/1.2178194]

The continued downscaling of semiconductor devices has resulted in functional materials being confined to nanometer size volumes, and they are, therefore, liable to be severely affected by atomistic defects in the material. This has fueled significant interest in the character of secondary defects and their long-range fields.^{1–3} In particular, the strain field associated with dislocations, and the strong interactions of dislocation cores with charge carriers and dopants have been investigated experimentally^{1,4} and theoretically.⁵ In the case of ferroelectric thin films, it was shown that the presence misfit dislocations (MDs) could severely impact ferroelectric and piezoelectric properties^{6–8} as well as the domain structure.⁹ Strong coupling of the polarization with the highly localized stress fields of MDs was shown to result in polarization gradients, capable of producing internal electric fields strong enough to suppress ferroelectricity and thus degrade physical properties.⁶

In addition to MDs, the microstructure of ferroelectric thin films contains invariably threading dislocations (TDs).^{10–13} There is now a clear consensus that the formation of MDs and TDs occurs by the glide of half-loops generated in response to misfit stresses at the interface, and that the final configuration consists of a MD segment lying in the interfacial plane bounded by two TD segments that thread from the interface to the deposit surface, in the manner first described by Matthews.¹⁴ While the effect of TDs on electrical properties in semiconductors is well documented,¹⁵ their role in ferroelectric films is yet to be fully understood. A preliminary study in epitaxial (001) $\text{Ba}_{0.6}\text{Sr}_{0.4}\text{TiO}_3$ films on (001) $0.29(\text{LaAlO}_3):0.35(\text{Sr}_2\text{TaAlO}_6)$ indicates that the improvement in the dielectric response upon annealing of the as-deposited samples might be attributed to reduction in the TD population.¹⁶ In this letter, building upon our prior thermodynamic formalism for MDs,⁶ we analyze the effect of TDs on the electrical properties of epitaxial ferroelectric thin films.

Examples of representative transmission electron microscopy (TEM) images obtained from a plan-view specimen of an epitaxial ferroelectric film are shown in Fig. 1. These data were obtained from a 300 nm thick (001) $\text{PbZr}_{0.2}\text{Ti}_{0.8}\text{O}_3$ (PZT) film grown by pulsed laser deposition using a 248 nm KrF excimer laser source onto a (001) single-crystal SrTiO_3 substrate at $T_G=600$ °C. The details of the growth parameters and TEM sample preparation are given elsewhere.^{8–13} Figures 1(a) and 1(b) are bright-field (BF) images obtained using diffraction vectors $\mathbf{g}=020$ and $\mathbf{g}=\bar{2}00$, respectively, with the beam direction close to $[001]$. Four different sets of TDs are present in the films and examples of these are indicated by the letters; A, B, C, and D, in Figs. 1(a) and 1(b). The TDs in Sets A and D have a line direction of $\xi=[001]$ and Burger’s vectors, \mathbf{b} , of $[010]$ and $[100]$, respectively. Thus, Set A exhibits very strong contrast in Fig. 1(a) with $\mathbf{g}=020$, but is out of contrast in Fig. 1(b) for which $\mathbf{g}=\bar{2}00$, and vice versa for Set D. These two sets constitute the majority of the TDs in the films (>90%) with a population density of approximately 10^{10} cm^{-2} but small numbers of defects from Sets B and C were observed as well. The TDs in

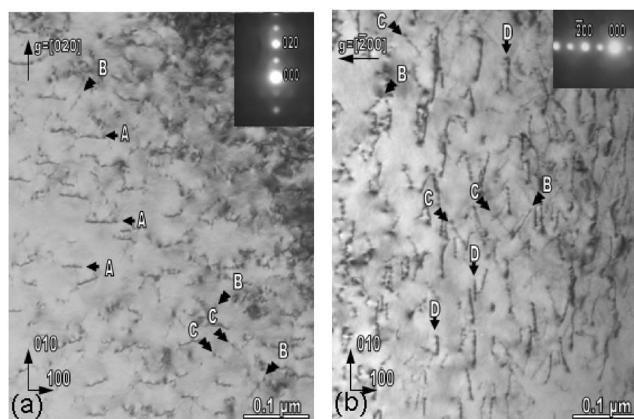


FIG. 1. BF plan-view TEM micrographs showing the dislocation microstructure near the surface of a 300 nm thick (001) PZT film grown on an (001) STO substrate.

^{a)} Author to whom correspondence should be addressed; electronic mail: p.alpay@ims.uconn.edu

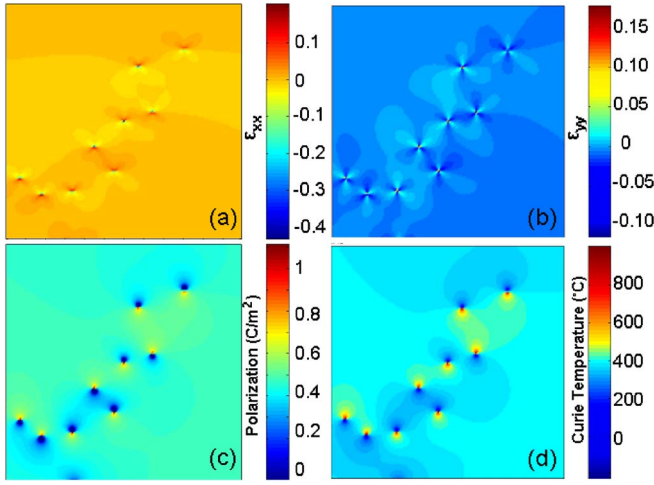


FIG. 2. (Color online) Theoretically calculated spatial variation of the total polarization-free in-plane components of the elastic strain ϵ_{xx} (a) and ϵ_{yy} (b) for randomly distributed TDs with $\mathbf{b}=[100]$ or $[\bar{1}00]$, plan view of out-of-plane polarization (c) and Curie temperature (d) variation. Areas shown in (a)–(d) represent a $60 \times 60 \text{ nm}^2$ area in the xy plane, 280 nm away from the interlayer interface. Individual elements in the simulations were taken to be $\sim 0.4 \text{ nm}$.

these sets had $\xi=\langle 111 \rangle$ and $\mathbf{b}=\langle 110 \rangle$. They exhibited weaker contrast than Sets A and D in images obtained using $\mathbf{g}=020$ or $\bar{2}00$, but much stronger contrast in images obtained using $\mathbf{g}=110$ or $1\bar{1}0$ (not shown). A more detailed analysis of the defect microstructure in this film is presented elsewhere.¹⁷

To model the effect of the TDs on the electrical properties, we have carried out theoretical calculations. TDs with $\mathbf{b}=[100]$ and $[\bar{1}00]$ were randomly distributed in an epitaxial 300 nm thick (001) PZT film on (001) STO with a population density of $\sim 10^{10} \text{ cm}^{-2}$, in accordance with the TEM micrographs in Fig. 1. The misfit between PZT and STO is -1.81% at T_G . This in-plane strain at T_G can be relaxed in 300 nm thick films via the formation of MDs resulting in an “effective” misfit strain¹⁸ of -0.048% at RT, determined using the Matthews-Blakeslee criteria¹⁹ with a critical thickness for dislocation formation of $\sim 9 \text{ nm}$. This effective in-plane misfit serves as the “background,” such that the total polarization-free elastic strain in the continuum limit is given by

$$\epsilon_{ij} = \epsilon_{ij}^M + \epsilon_{ij}^{\text{TD}}, \quad (1)$$

where ϵ_{ij}^M is the effective misfit and $\epsilon_{ij}^{\text{TD}}$ is the self-strain of a TD. We note that we neglect the self-strain of the MDs in our analysis although the effective misfit strain does contain their contribution in the relaxation of the misfit at T_G . This is a reasonable approximation for films with a film thickness well above the critical thickness for MD formation. The self-strain of MDs would certainly alter the total strain state near the film-substrate interface on which MDs form. Although the strength of the strain field of the MDs fades quickly in accordance with St. Venant’s principle, this would become crucial for film thicknesses below $\sim 15 \text{ nm}$.^{6,8} Using the spatial variation of $\epsilon_{ij}^{\text{TD}}$,²⁰ the strain state of a ferroelectric film containing TDs can be mapped. We define a Cartesian coordinate axis such that $x \perp [100]_{\text{PZT}}$, $y \perp [010]_{\text{PZT}}$, and $z // [001]_{\text{PZT}}$ and note that the dislocation line is parallel to the z direction. In Figs. 2(a) and 2(b), we show the strain

distribution due to TDs in PZT on STO in the xy plane at RT and at a thickness of 280 nm, sufficiently away from the film-substrate interface.

The strain field can then be incorporated into the Landau–Devonshire (LD) potential to determine the polarization distribution such that

$$\bar{F}(P, T, \epsilon_{ij}^T) = F(P, T) + F_{\text{Elastic}}(\epsilon_{ij}^T), \quad (2)$$

where

$$F(P, T) = F_0 + \alpha_1 P^2 + \alpha_{11} P^4 + \alpha_{111} P^6, \quad (3)$$

is the LD free energy of a single-domain ferroelectric with a uniform polarization P along the z axis, and α_1 , α_{11} , and α_{111} are the dielectric stiffness coefficients. The temperature dependence of α_1 is given by the Curie–Weiss law, $\alpha_1 = (T - T_C)/2\epsilon_0 C$, where T_C and C are the Curie–Weiss temperature and constant, respectively, and ϵ_0 is the permittivity of free space.

The last term in Eq. (2) is the total elastic energy given by

$$F_{\text{Elastic}} = \frac{1}{2} \epsilon_{ij}^T \cdot C_{ijkl} \cdot \epsilon_{kl}^T, \quad (4)$$

where C_{ijkl} are the elastic moduli of the film. ϵ_{ij}^T is the total elastic strain:⁹

$$\epsilon_{ij}^T = \epsilon_{ij}^M + \epsilon_{ij}^{\text{TD}} + \epsilon_{ij}^0, \quad (5)$$

where $\epsilon_{ij}^0 = P_k \cdot Q_{ijkl} \cdot P_l$ is the self-strain tensor of the paraelectric-to-ferroelectric phase transformation and Q_{ijkl} are the electrostrictive coefficients.

The thermodynamic analysis results in a polarization and Curie temperature variation due to the spatial dependence of the strain field around the TDs [Figs. 2(c) and 2(d)]. The spontaneous polarization P_0 is given by the equation of state, $\partial \bar{F} / \partial P = 0$ and local T_C can be determined by setting the (renormalized) first Landau coefficient α_1 equal to zero. In regions where the strain field is negative (compressive strain), we see an increase in T_C and a commensurate improvement in the local polarization. On the other hand, in tensile regions T_C may drop to below RT, resulting in zero local polarization. Local variations in T_C result in a diffuse, or “smeared,” ferroelectric-paraelectric transformation instead of the sharp transformation in defect-free single crystals. We note that the polarization distribution around the TDs is in complete agreement with the results for piezoelectric wurtzite GaN.²¹

To fully understand the effect of TDs on the electrical properties, we must go beyond the thermodynamic formalism and incorporate electrostatic interactions between polarization dipoles. This can be achieved via the Maxwell’s relations:²²

$$\nabla \times \mathbf{E}_D = 0; \quad \nabla \cdot \mathbf{E}_D = (1/\epsilon_0)(\rho - \nabla \cdot \mathbf{P}), \quad (6)$$

where \mathbf{E}_D is an internal field due to polarization fluctuations and ρ is the density of free charges. In Fig. 3(a), we show a schematic representation of TDs and MDs in an epitaxial film. The dislocation line of a TD is parallel to the z direction, the easy axis of the polarization. As shown in Fig. 3(b), along infinitesimally small z -axis-oriented strips, polarization along the z direction is divergence free, i.e., $\nabla \cdot \mathbf{P} = 0$, although the magnitude of the polarization does change along the x and y axes as one moves away from the dislocation

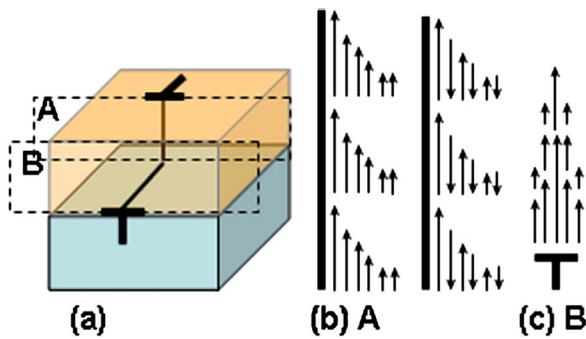


FIG. 3. (Color online) (a) Schematic configuration of a threading and misfit segments of a dislocation half-loop in an epitaxial ferroelectric film, (b) schematic variation of the polarization near a TD in the AA plane showing two possible configurations, and (c) around a MD in the BB plane, along the z axis, direction of easy polarization.

line. In the case of an insulating ferroelectric film and charge-neutral dislocation core, this implies that this configuration should not produce an internal (depolarizing) field along the z axis. This is in agreement with the electrostatic analysis of edge dislocations with a dislocation line along the c axis of piezoelectric GaN.²¹ Another divergence-free arrangement of dipoles would consist of antiparallel polarization variation near TDs as shown in Fig. 3(b) that results from minimization of the dipole-dipole electrostatic interactions.²³

In contrast, for MDs where the polarization vector is perpendicular to the dislocation line, the electrostatic conditions are quite different [Fig. 3(c)]. We have shown that the out-of-plane polarization around the MDs exhibits a dramatic divergence along the z direction due to the varying strain fields starting from the interface.⁶ This configuration, especially in the vicinity of the MD cores, results in internal electric fields sufficient enough to suppress ferroelectricity²⁴ in a region extending around 10 nm from the dislocation core.⁶ The severe degradation in the electrical properties due to these dead regions has been discussed in detail both theoretically⁶ and experimentally.⁸

Comparing the two different electrostatic conditions for MDs and TDs, it is apparent that the effect of TDs on electrical properties is not as detrimental as that of MDs. In Ref. 16, the annealing of BST films resulted in a slight increase ($\sim 10\%$) in the dielectric properties of the films. We note that the compressive regions of the TDs have a higher transition temperature T_C [Fig. 2(d)] that would lower the overall dielectric constant of the film.²⁵ Thus, the improvement in the dielectric response can be related to the reduction of the TD density through the elimination of their compressive regions.

In conclusion, the effect of TDs on ferroelectric properties has been analyzed using thermodynamic models and basic electrostatic considerations for a TD configuration with a dislocation line perpendicular to the film-substrate interface, i.e., in the direction of the spontaneous polarization. We show that although the phase transformation characteristics of ferroelectric films containing TDs are modified, resulting in a diffuse ferroelectric phase transformation due to local strain gradients, these defects do not have as profound an effect on the electrical properties as the MDs. With larger film thicknesses, the MDs will affect only the region close to the interface, while TDs will still give rise to the same

smearing of the phase transformation temperature unless there are radical variations in TD density with distance from the interface. For thinner films, the overlapping of the stress fields of MDs and TDs may result in polarization variations throughout the entire volume of the material, leading to complete suppression of ferroelectricity. We note that for the case of TDs whose dislocation lines do not lie parallel to the direction of the spontaneous polarization, we would also expect the generation of polarization gradients. This would result in a more significant reduction in the ferroelectric properties, similar to the case of degradation of ferroelectricity near MDs.

The work at UConn was supported by the National Science Foundation (NSF) under Grant No. DMR-0132918 and by the American Chemical Society, The Petroleum Research Fund. The authors thank R. Ramesh for many useful discussions and for providing the samples used in this study. The authors also thank A. L. Vasiliev for his help with the TEM analysis.

¹M. J. Hytch, J.-L. Putaux, and J.-M. Penisson, *Nature (London)* **423**, 270 (2003).

²M.-W. Chu, I. Szafraniak, R. Scholz, C. Harnagea, D. Hesse, M. Alexe, and U. Gösele, *Nat. Mater.* **3**, 87 (2003).

³D. A. Muller, N. Nakagawa, A. Ohtomo, J. L. Grazul, and H. Y. Hwang, *Nature (London)* **430**, 657 (2004).

⁴A. Maiti, M. F. Chisholm, S. J. Pennycook, and S. T. Pantelides, *Phys. Rev. Lett.* **77**, 1306 (1996).

⁵L. Lymerakis, J. Neugebauer, M. Albrecht, T. Remmele, and H. P. Strunk, *Phys. Rev. Lett.* **93**, 196401 (2004).

⁶S. P. Alpay, I. B. Misirlioglu, V. Nagarajan, and R. Ramesh, *Appl. Phys. Lett.* **85**, 2044 (2004).

⁷D. Balzar, P. A. Ramakrishnan, and A. M. Hermann, *Phys. Rev. B* **70**, 092103 (2004); D. Balzar, P. A. Ramakrishnan, P. Spagnol, S. Mani, A. M. Hermann, and M. A. Matin, *Jpn. J. Appl. Phys., Part 1* **41**, 6628 (2002).

⁸V. Nagarajan, I. B. Misirlioglu, C. L. Jia, H. Kohlstedt, R. Waser, S. P. Alpay, and R. Ramesh, *Appl. Phys. Lett.* **86**, 192910 (2005).

⁹S. Y. Hu, Y. L. Li, and L. Q. Chen, *J. Appl. Phys.* **94**, 2542 (2003).

¹⁰T. Suzuki, Y. Nishi, and M. Fujimoto, *Philos. Mag. A* **79**, 2461 (1999).

¹¹C. J. Lu, L. A. Bendersky, K. Chang, and I. Takeuchi, *J. Appl. Phys.* **93**, 512 (2003).

¹²H. P. Sun, W. Tian, X. Q. Pan, J. H. Haeni, and D. G. Schlom, *Appl. Phys. Lett.* **84**, 3298 (2004).

¹³I. B. Misirlioglu, A. L. Vasiliev, M. Aindow, S. P. Alpay, and R. Ramesh, *Appl. Phys. Lett.* **84**, 1742 (2004).

¹⁴J. W. Matthews, *J. Vac. Sci. Technol.* **12**, 126 (1975).

¹⁵See for example: L. A. Kolodziejzski, R. L. Gunshor, and A. V. Nurmikko, *Annu. Rev. Mater. Sci.* **25**, 711 (1995); S. Nakamura, *Science* **281**, 956 (1998).

¹⁶C. L. Canedy, H. Li, S. P. Alpay, L. Salamanca-Riba, A. L. Roytburd, and R. Ramesh, *Appl. Phys. Lett.* **77**, 1695 (2000).

¹⁷I. B. Misirlioglu, A. L. Vasiliev, S. P. Alpay, M. Aindow, and R. Ramesh, *J. Mater. Sci.* **41**, 697 (2006).

¹⁸J. S. Speck and W. Pompe, *J. Appl. Phys.* **76**, 466 (1994).

¹⁹J. W. Matthews and A. E. Blakeslee, *J. Cryst. Growth* **27**, 118 (1974).

²⁰We do not include these relations for brevity and refer the reader to J. P. Hirth and J. Lothe, *Theory of Dislocations*, 2nd ed. (Wiley, New York, 1982).

²¹C. Shi, P. M. Asbeck, and E. T. Yu, *Appl. Phys. Lett.* **74**, 573 (1999).

²²M. E. Lines and A. M. Glass, *Principles and Application of Ferroelectrics and Related Materials* (Clarendon, Oxford, 1977).

²³Upon cooling from T_G , regions with higher T_C will be spontaneously polarized, whereas in regions where ferroelectricity sets in later, the internal field of the pre-existing polarized areas may impose an antiparallel arrangement. In an electroded parallel-plate sample, charge compensation at the electrode-film interfaces may result in a parallel alignment of polarization.

²⁴A. M. Bratkovsky and A. P. Levanyuk, *Phys. Rev. B* **66**, 184109 (2002).

²⁵Z. G. Ban and S. P. Alpay, *J. Appl. Phys.* **91**, 9288 (2002).